

# Acetonitrile-Based Electrolytes for Rechargeable Zinc Batteries

Ahmed S. Etman,\* Marco Carboni, Junliang Sun, and Reza Younesi\*

Herein, Zn plating–stripping onto metallic Zn using a couple of acetonitrile (AN)-based electrolytes (0.5 M Zn(TFSI)<sub>2</sub>/AN and 0.5 M Zn(CF<sub>3</sub>SO<sub>3</sub>)<sub>2</sub>/AN) is studied. Both electrolytes show a reversible Zn plating/stripping over 1000 cycles at different applied current densities varying from 1.25 to 10 mA cm<sup>-2</sup>. The overpotentials of Zn plating–stripping over 500 cycles at constant current of 1.25 and 10 mA cm<sup>-2</sup> are ±0.05 and ±0.2 V, respectively. X-ray photoelectron spectroscopy analysis reveals that no decomposition product is formed on the Zn surface. The anodic stability of four different current collectors of aluminum foil (Al), carbon-coated aluminum foil (C/Al), TiN-coated titanium foil (TiN/Ti), and multiwalled carbon nanotube paper (MWCNT-paper) is tested in both electrolytes. As a general trend, the current collectors have a higher anodic stability in Zn(TFSI)<sub>2</sub>/AN compared with Zn(CF<sub>3</sub>SO<sub>3</sub>)<sub>2</sub>/AN. The Al foil displays the highest anodic stability of ≈2.25 V versus Zn<sup>2+</sup>/Zn in Zn(TFSI)<sub>2</sub>/AN electrolyte. The TiN/Ti shows a comparable anodic stability with that of Al foil, but its anodic current density is higher than Al. The promising reversibility of the Zn plating/stripping combined with the anodic stability of Al and TiN/Ti current collectors paves the way for establishing highly reversible Zn-ion batteries.

batteries.<sup>[13–17]</sup> Among them, nonaqueous Zn batteries are interesting to consider, as metallic zinc anode has a higher volumetric capacity compared with metallic Mg and Ca anodes (5851 mAh cm<sup>-3</sup> for Zn compared with 3833 and 2073 mAh cm<sup>-3</sup> for Mg and Ca, respectively).<sup>[18–21]</sup> Furthermore, the Zn<sup>2+</sup> showed a reasonable activation energy barrier for its diffusion in many cathodes (e.g., Prussian blue analogue, V<sub>2</sub>O<sub>5</sub>, ZnAl<sub>x</sub>Co<sub>2-x</sub>O<sub>4</sub>, and FePO<sub>4</sub>), which provides opportunities for developing a high capacity nonaqueous Zn batteries.<sup>[13,17,19,22–25]</sup> Recent studies have also shown that carbon-based materials can be used, for example, graphite can be used as a cathode material for the rechargeable Zn batteries.<sup>[26–28]</sup>

The electrochemical reduction potential of Zn<sup>2+</sup> [-0.76 vs standard hydrogen electrode (SHE)] is, however, higher than that of Mg<sup>2+</sup> (-2.37 V vs SHE) and Ca<sup>2+</sup> (-2.87 vs SHE),<sup>[19,29,30]</sup> which makes it less interesting in terms of cell voltage.

Nevertheless, the relatively high electrochemical potential of Zn<sup>2+</sup>/Zn leaves metallic zinc within the electrochemical stability window of most aprotic electrolytes. This means there is no need of formation of the solid-electrolyte-interphase (SEI) on metallic zinc, rendering possibility for high-rate electrochemical plating–stripping of Zn<sup>2+</sup>/Zn. The formation of SEI on metallic Ca and Mg batteries is indeed one major challenge to achieve reversible plating–stripping at room temperature.<sup>[30,31]</sup>

Burrell et al.<sup>[17]</sup> investigated different nonaqueous Zn electrolytes and reported very promising results regarding high reversibility of Zn plating–stripping and ionic conductivity in acetonitrile

## 1. Introduction

The research interest in rechargeable batteries and supercapacitors keeps growing due to their application in a variety of technologies such as portable electronic devices, hybrid vehicles, grid storage, and so on.<sup>[1–8]</sup> Li-ion batteries have been developed to commercial application over last 30 years;<sup>[9–12]</sup> however, rechargeable nonaqueous batteries based on multivalent ions (e.g., Mg<sup>2+</sup>, Ca<sup>2+</sup>, and Zn<sup>2+</sup>) have attracted a lot of interest in the last few years due to their abundancy in nature and their potential to provide a reasonable energy density compared with the state-of-art Li-ion

Dr. A. S. Etman, Prof. J. Sun  
Department of Materials and Environmental Chemistry (MMK)  
Stockholm University  
Stockholm SE-10691, Sweden  
E-mail: ahmed.s.etman@alexu.edu.eg

Dr. A. S. Etman  
Department of Chemistry  
Faculty of Science  
Alexandria University  
P.O. Box 426, Ibrahimia, Alexandria 21321, Egypt

Dr. M. Carboni, Prof. R. Younesi  
Ångström Advanced Battery Centre  
Department of Chemistry-Ångström Laboratory  
Uppsala University  
Box 538, Uppsala SE-75121, Sweden  
E-mail: reza.younesi@kemi.uu.se

Prof. J. Sun  
College of Chemistry and Molecular Engineering  
Peking University  
Yihyuan Road 5, Beijing 100871, China

The ORCID identification number(s) for the author(s) of this article can be found under <https://doi.org/10.1002/ente.202000358>.

© 2020 The Authors. Published by Wiley-VCH GmbH. This is an open access article under the terms of the Creative Commons Attribution License, which permits use, distribution and reproduction in any medium, provided the original work is properly cited.

DOI: 10.1002/ente.202000358

(AN)-based electrolytes. Moreover, they did not observe Zn-dendrite growth when  $\text{Zn}(\text{TFSI})_2/\text{AN}$  or  $\text{Zn}(\text{CF}_3\text{SO}_3)_2/\text{AN}$  was used as the electrolyte. However, they used three electrode setup with Pt disk as working electrode to study the efficiency of plating–stripping and the anodic decomposition potential of electrolytes.<sup>[17]</sup> Recently, Zhang et al. studied the Zn plating–stripping in 1 M  $\text{Zn}(\text{TFSI})_2/\text{AN}$  using symmetric Zn|Zn cells at current densities ranging between 0.1 and 5 mA cm<sup>-2</sup>.<sup>[26]</sup> Therefore, there is a need to explore the plating–stripping in  $\text{Zn}(\text{CF}_3\text{SO}_3)_2/\text{AN}$  using symmetric Zn|Zn cells, and also investigate the plating–stripping at much higher applied current densities.

To approach the development of practical nonaqueous Zn batteries, we herein report overpotential and rate capacity of plating–stripping of  $\text{Zn}^{2+}/\text{Zn}$  on metallic Zn electrodes using two different electrolyte salts of  $\text{Zn}(\text{TFSI})_2$  or  $\text{Zn}(\text{CF}_3\text{SO}_3)_2$  (can also be referred to as TFSI and Triflate, respectively) dissolved in AN. The surface of the Zn metal was analyzed by X-ray photoelectron spectroscopy (XPS) after plating–stripping cycles. Furthermore, the anodic decomposition potential of the aforementioned electrolytes on different current collectors such as aluminum foil (Al), carbon-coated aluminum foil (C/Al), TiN-coated titanium foil (TiN/Ti),

and multiwalled carbon nanotube paper (MWCNT-paper) is herein investigated.

## 2. Results and Discussion

Figure 1 shows galvanostatic plating–stripping of symmetrical Zn|Zn cells in 0.5 M  $\text{Zn}(\text{CF}_3\text{SO}_3)_2/\text{AN}$  or 0.5 M  $\text{Zn}(\text{TFSI})_2/\text{AN}$  electrolytes targeting charge of 1.47 C cm<sup>-2</sup>. Both low and high applied current densities of 1.25 and 10 mA cm<sup>-2</sup> can provide a stable long-term plating–stripping; however, the electrochemical performance is slightly different depending on the choice of zinc salt. When a low current density of 1.25 mA cm<sup>-2</sup> is applied (see Figure 1a), the cell with  $\text{Zn}(\text{TFSI})_2/\text{AN}$  electrolyte requires slightly higher overpotential during the initial cycles (about 0.30 V), compared with the cell containing  $\text{Zn}(\text{CF}_3\text{SO}_3)_2/\text{AN}$  electrolyte (about 0.10 V in the initial cycles and 0.04 V after about 23 cycles). This slightly higher overpotential for  $\text{Zn}(\text{TFSI})_2/\text{AN}$  electrolyte is observable—though becomes smaller—in long-term cycling as well, in particular after about 16 plating–stripping cycles the overpotential of  $\text{Zn}(\text{TFSI})_2/\text{AN}$  is dropped and stabilized at about 0.07 V

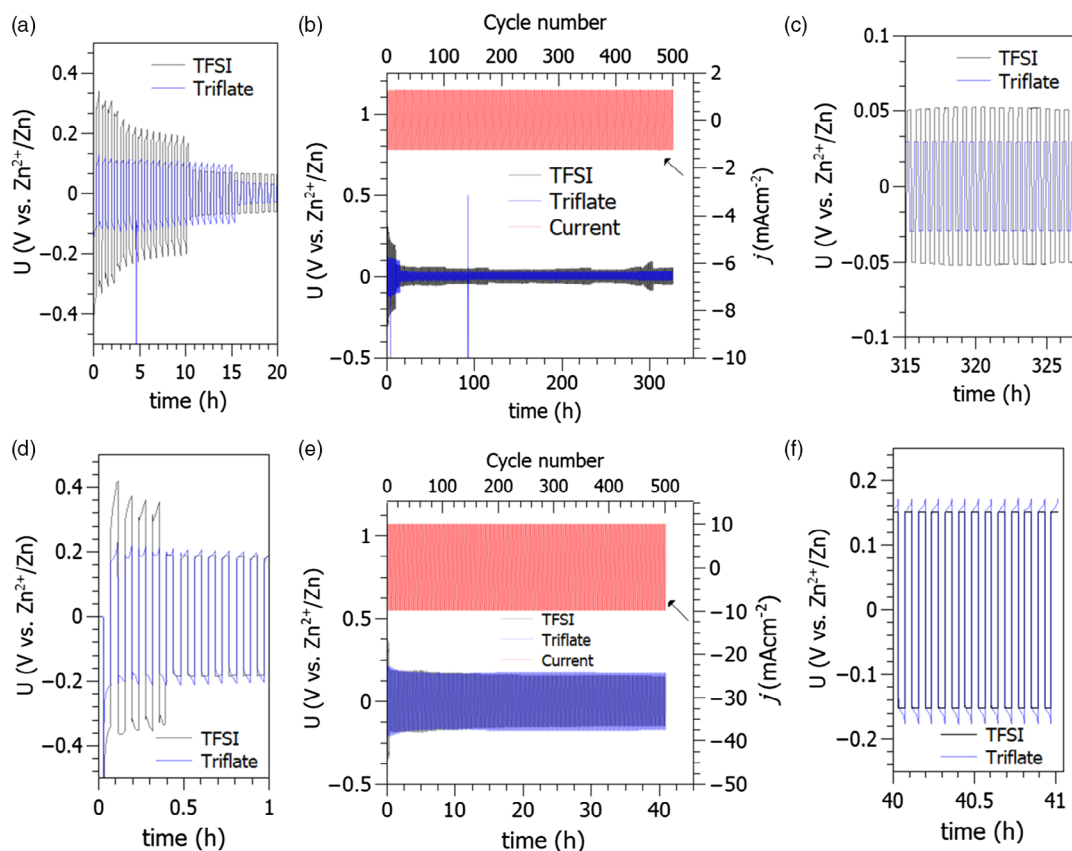


**Figure 1.** Galvanostatic plating–stripping in symmetrical Zn|Zn cells at constant current densities targeting a charge of 1.47 C cm<sup>-2</sup> in 0.5 M  $\text{Zn}(\text{CF}_3\text{SO}_3)_2/\text{AN}$  (blue) or 0.5 M  $\text{Zn}(\text{TFSI})_2/\text{AN}$  (black): a) voltage/time profile for the first few plating–stripping cycles at low applied current density of 1.25 mA cm<sup>-2</sup>, and b) the corresponding long-term cycling for 500 cycles. c) Voltage/time profile for the last few plating–stripping cycles at low applied current density of 1.25 mA cm<sup>-2</sup>, d) voltage/time profile for the first few plating–stripping cycles at high applied current density of 10 mA cm<sup>-2</sup>, and e) the corresponding long-term cycling for 500 cycles. f) Voltage/time profile for the last few plating–stripping cycles at high applied current density of 10 mA cm<sup>-2</sup>.

(see Figure 1b,c). The latter overpotential result is more superior than those reported earlier in a symmetrical Zn|Zn cells with 1 M Zn(TFSI)<sub>2</sub>/AN,<sup>[26]</sup> as the overpotential was stabilized at about 0.09 V under current density of about 1 mA cm<sup>-2</sup>. However, our results in 0.5 M Zn(TFSI)<sub>2</sub>/AN showed wider variations in overpotential of the first few cycles as compared with others,<sup>[26]</sup> which might be attributed to the difference in the activation of the Zn surface in 0.5 and 1 M Zn(TFSI)<sub>2</sub>.

Similarly, for the higher current density of 10 mA cm<sup>-2</sup>, the cell with Zn(TFSI)<sub>2</sub>/AN electrolyte displayed slightly higher overpotential in the very few initial cycles ( $\approx 4$  cycles; see Figure 1d), but the overpotential becomes stable at about 0.20–0.15 V for both cells over 500 cycles as shown in Figure 1e,f. These values of overpotentials at high current densities in Zn(TFSI)<sub>2</sub>/AN are in a good agreement with the previous report.<sup>[28]</sup> Previous reports approved that the morphology of the plated Zn is dendrite free even at high current density; in addition, the purity of

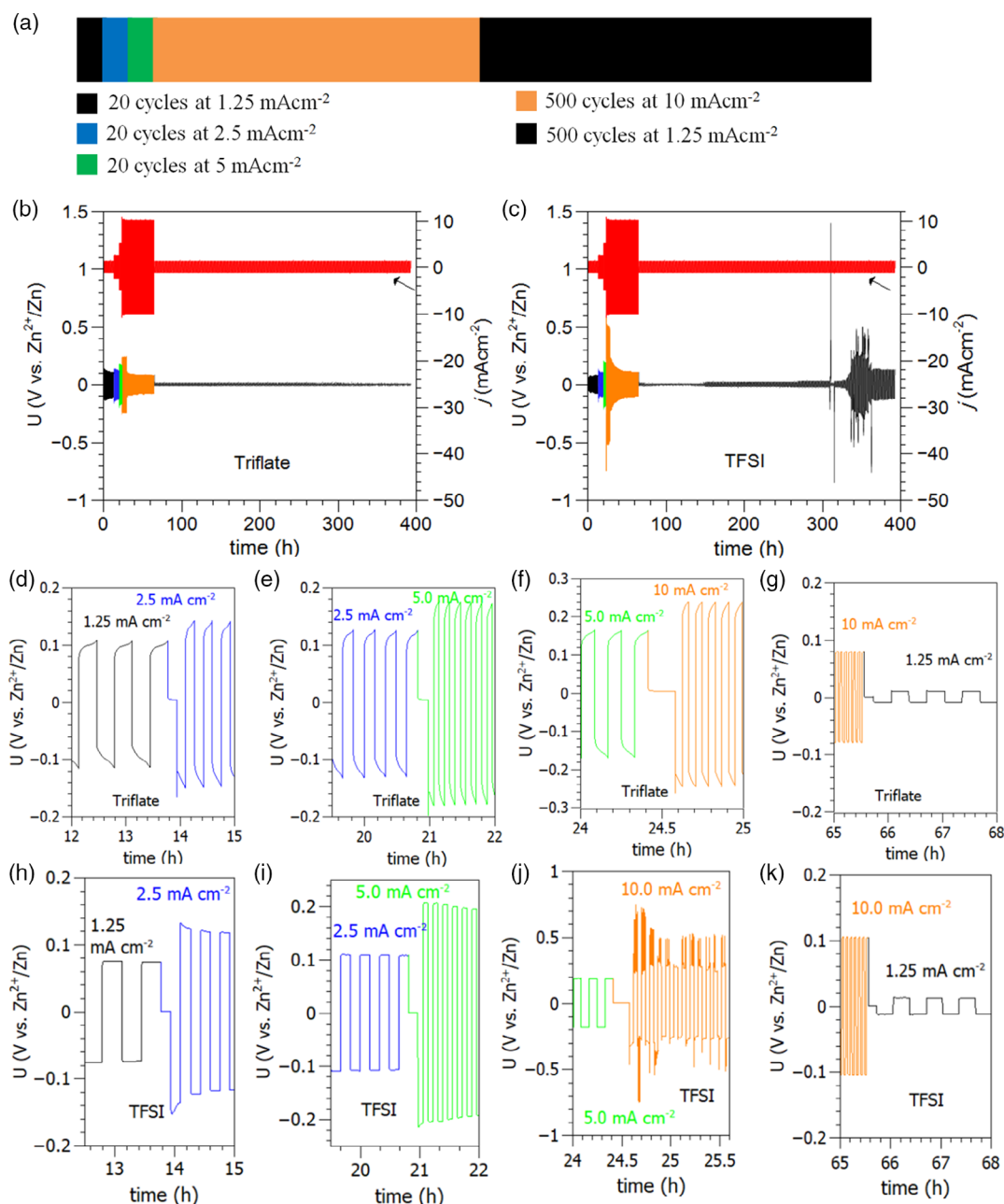


**Figure 2.** Galvanostatic plating–stripping in symmetrical Zn|Zn cells at different applied current densities varying from 1.25 to 10 mA cm<sup>-2</sup> targeting a charge of 1.47 C cm<sup>-2</sup>: a) schematic presentation for the cycling protocol; b,c) voltage/time profile in cells with 0.5 M Zn(CF<sub>3</sub>SO<sub>3</sub>)<sub>2</sub>/AN and 0.5 M Zn(TFSI)<sub>2</sub>/AN, respectively. d–g) Enlarged voltage/time profiles for the transition between different current densities in Zn(CF<sub>3</sub>SO<sub>3</sub>)<sub>2</sub>/AN. h–k) Enlarged voltage/time profiles for the transition between different current densities in Zn(TFSI)<sub>2</sub>/AN.

the deposited Zn is very high and its degree of crystallinity is inversely proportional to the applied current density of the plating.<sup>[17,26,28]</sup>

The coulombic efficiencies of plating–stripping at both low and high applied current densities are >99.8% (see Figure S1a,b, Supporting Information), which reflect the high reversibility of plating–stripping in both electrolytes. It worth mentioning that this high efficiency of plating–stripping was obtained in a number of cells with similar parameters, showing high reproducibility of the results (e.g., Figure S1, Supporting Information, to compare with Figure 1). Notably, in Figure S1c,d, Supporting Information, the overpotential of Zn(TFSI)<sub>2</sub>/AN electrolyte is comparable with that of Zn(CF<sub>3</sub>SO<sub>3</sub>)<sub>2</sub>/AN electrolyte, indicating the slight difference in the overpotential of the initial cycles might come from the traces of passive oxide on Zn metal.

The rate capability test for plating–stripping was performed at different current densities of 1.25, 2.5, 5, and 10 mA cm<sup>-2</sup>, targeting charge of 1.47 C cm<sup>-2</sup>. Figure 2a shows a schematic presentation for the cycling protocol. As shown in Figure 2b,c, the plating–stripping overpotential increases as the current density increases; however, it did not exceed ±0.5 V over more than 300 h of cycling. The variation of the overpotential can be better observed from the enlarged voltage/time profiles for the transition between a given current density and another (see Figure 2d–g and Figure 2h–k for the Zn(CF<sub>3</sub>SO<sub>3</sub>)<sub>2</sub>/AN and Zn(TFSI)<sub>2</sub>/AN, respectively). However, after about 350 h (about 800 cycles) plating–stripping, the cell with Zn(TFSI)<sub>2</sub>/AN started to show an increase in the overpotential (≈0.45 V and stabilized after few cycles at 0.15 V). This increase in the overpotential can be due to cell failure or changes in the surface upon long-term plating–stripping at low current density (see XPS discussion later). Overall, the results in Figure 1 and 2 show that both Zn(CF<sub>3</sub>SO<sub>3</sub>)<sub>2</sub>/AN and Zn(TFSI)<sub>2</sub>/AN electrolytes could be considered as superior electrolytes for Zn plating–stripping

on metallic Zn; however, Zn(CF<sub>3</sub>SO<sub>3</sub>)<sub>2</sub>/AN outperforms Zn(TFSI)<sub>2</sub>/AN especially at low plating–stripping rates. The pretreatment of Zn foil with 3% HCl showed a slight improvement in the plating–stripping for the cells containing Zn(TFSI)<sub>2</sub>/AN (see Note S1 and Figure S2, Supporting Information). In particular, the overpotentials during long-term plating–stripping remained steady even at low plating–stripping current density (see Figure S2c, Supporting Information); however, the overpotentials were relatively higher than those obtained in the Zn(CF<sub>3</sub>SO<sub>3</sub>)<sub>2</sub>/AN. This enhancement reflects that the surface of the pristine Zn plays an important role in the long-term plating–stripping performance, especially in the Zn(TFSI)<sub>2</sub>/AN.

XPS measurement was performed to analyze any possible surface layer formation on Zn metal electrodes. The Zn 2p, O 1s, and C 1s spectra shown in Figure 3 indicate that the surface composition of the cycled Zn electrode in 0.5 M Zn(TFSI)<sub>2</sub>/AN is very similar to the pristine Zn electrode; therefore, no major decomposition products formed on the surface of Zn metal. However, the peaks observed at 688.9, 399.5, 169.1, and 293 eV in the F 1s, N 1s, S 2p, and C 1s spectra, respectively, of the cycled sample disclose that some of Zn(TFSI)<sub>2</sub> salt remained—but not decomposed—on the surface of Zn electrode, though the electrode was rinsed with pure AN before XPS measurement.<sup>[32]</sup> The ratios between the amounts of the elements on the surface were 5.5 for F/N, 3.7 for F/S, and 1.5 for S/N which are close to the theoretical ratio of 6, 3, and 2, respectively, expected for TFSI (-N(SO<sub>2</sub>CF<sub>3</sub>)<sub>2</sub>) anion.<sup>[26,28]</sup> This also indicates that the salt did not decompose and just rather remained attached to the surface of Zn metal. The total amounts of F, S, and N originated from the salt species are below 15 atomic% which did not block out signals from the Zn substrate. Therefore, one possible reason for the relatively lower performance of Zn(TFSI)<sub>2</sub>/AN cells as compared with Zn(CF<sub>3</sub>SO<sub>3</sub>)<sub>2</sub>/AN might be the accumulation of TFSI on the

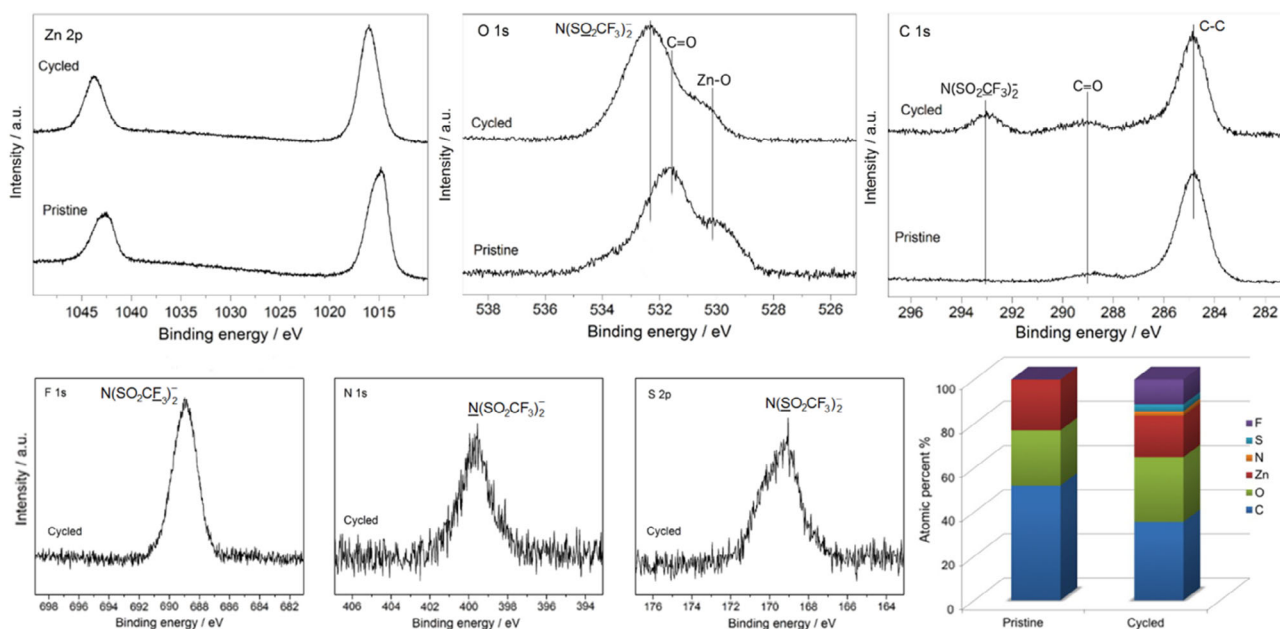


**Figure 3.** XPS spectra of pristine Zn metal electrode and Zn metal electrode cycled in a symmetrical cell with electrolyte of 0.5 M Zn(TFSI)<sub>2</sub>/AN.

surface, which changes the surface especially at low current density of plating–stripping.

To use any of the aforementioned electrolytes in full-cell Zn batteries, they need to be stable at high potential where an

applied cathode performs. Burrell et al.<sup>[17]</sup> used a platinum electrode to measure the anodic stability of these electrolytes, leading to high stability up to 3.6–3.8 V (vs Zn/Zn<sup>2+</sup>); however, the anodic stability on practical current collectors was not

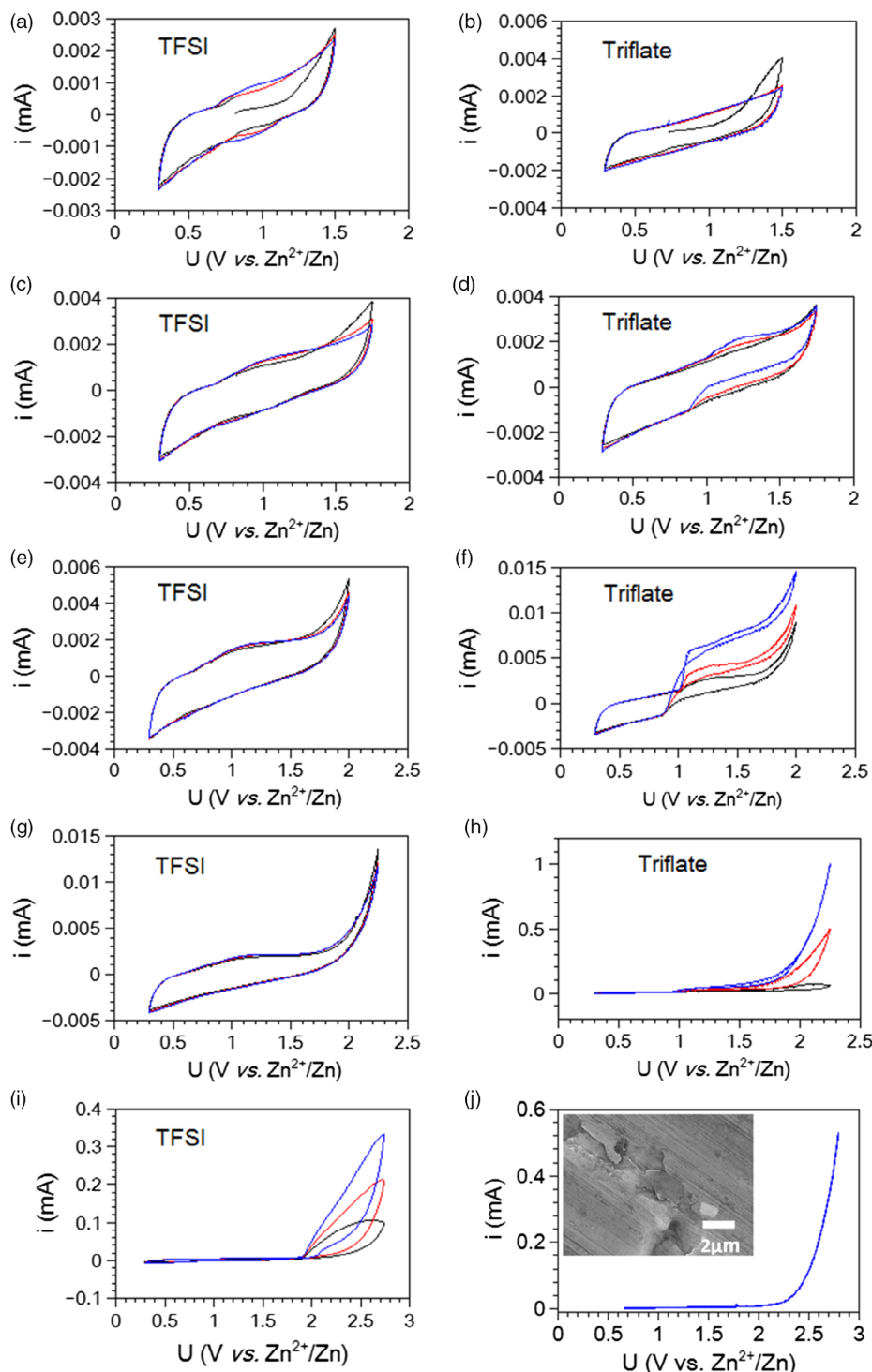


**Figure 4.** Electrochemical stability of Al-current collector in AN-based electrolytes: a,c,e,g,i) CVs in 0.5 M Zn(TFSI)<sub>2</sub>/AN; b,d,f,h) CVs in 0.5 M Zn(CF<sub>3</sub>SO<sub>3</sub>)<sub>2</sub>/AN. The black, red, and blue curves represent first, second, and third scans; respectively. j) LSV on Al-current collector in 0.5 M Zn(TFSI)<sub>2</sub>/AN, and the inset SEM image showing surface of Al after the LSV. The scan rate in all CV and LSV experiments was 10 mV s<sup>-1</sup>.

discussed. Later on, it was shown that Ti foil can be used as a current collector, and its stability in  $\text{Zn}(\text{TFSI})_2/\text{AN}$  is higher than that in  $\text{Zn}(\text{CF}_3\text{SO}_3)_2/\text{AN}$ .<sup>[28]</sup> We therefore conducted electrochemical measurements on some other current collectors which could be used in a full-cell setup. Cyclic voltammetry (CV) was conducted to explore the anodic stability of the Al current collector in  $\text{Zn}(\text{CF}_3\text{SO}_3)_2/\text{AN}$  and  $\text{Zn}(\text{TFSI})_2/\text{AN}$  electrolytes. Figure 4b,d,f shows cyclic voltammograms (CVs) using Al foil as the working electrode in  $\text{Zn}(\text{CF}_3\text{SO}_3)_2/\text{AN}$  electrolyte. The results disclose that the anodic charge in the cell with  $\text{Zn}(\text{CF}_3\text{SO}_3)_2/\text{AN}$  increased upon cycling even at relatively low upper cutoff voltage of 1.75 or 2.0 V versus  $\text{Zn}^{2+}/\text{Zn}$ , indicating the low anodic stability of Al in this electrolyte. Notably, when the upper cutoff voltage was raised further to 2.25 V, the anodic charge increases tremendously (see Figure 4h). This poor anodic stability in  $\text{Zn}(\text{CF}_3\text{SO}_3)_2/\text{AN}$  is in agreement with the previous report,<sup>[28]</sup> and can be attributed to the decomposition of the electrolyte and/or enhancement of the current collector oxidation in the presence of Triflate anion.

On the contrary, CVs of Al in  $\text{Zn}(\text{TFSI})_2/\text{AN}$  displayed more promising anodic stability up to  $\approx 2.25$  V (see Figure 4a,c,e,g). However, when the upper cutoff voltage was raised to 2.5 or 2.75 V, the anodic charge started to increase (see Figure 4i). To further enrich the picture, linear sweep voltammetry (LSV) was used to Al foil in  $\text{Zn}(\text{TFSI})_2/\text{AN}$  electrolyte, where the potential was swept from open-circuit potential (OCP) to 2.8 V (see Figure 4j). The current remained almost constant until the cell reached the potential of 2.25 V, and then it increased linearly with the potential, indicating the decomposition of the electrolyte and/or the corrosion of the Al current collector. The scanning electron microscopy (SEM) images confirmed the corrosion of the Al after the LSV test (inset of Figure 4j). Moreover, the anodic stability of other current collectors such as C/Al, TiN/Ti, and MWCNT-paper was investigated in  $\text{Zn}(\text{TFSI})_2/\text{AN}$  and  $\text{Zn}(\text{CF}_3\text{SO}_3)_2/\text{AN}$  electrolytes (Figure S3–S5, Supporting Information). The results showed that Al is the most stable collector in both electrolytes compared with C/Al and MWCNT-paper. TiN/Ti shows an anodic current density higher than that of Al foil, but its anodic stability is comparable with Al. This observation suggests that TiN/Ti is another applicable current collector for nonaqueous Zn batteries. Recent studies have shown that the anodic dissolution of the Al current collector can be suppressed using a highly concentrated Li-TFSI electrolyte.<sup>[33]</sup> Therefore, future studies are needed to explore the possibility of improving the anodic stability of the current collectors in highly concentrated  $\text{Zn}(\text{TFSI})_2/\text{AN}$  and  $\text{Zn}(\text{CF}_3\text{SO}_3)_2/\text{AN}$ .

### 3. Conclusion

In summary,  $\text{Zn}^{2+}/\text{Zn}$  can be reversibly plated–stripped on metallic Zn in both 0.5 M  $\text{Zn}(\text{TFSI})_2/\text{AN}$  and 0.5 M  $\text{Zn}(\text{CF}_3\text{SO}_3)_2/\text{AN}$  electrolytes. The plating–stripping coulombic efficiency was  $>99.8\%$  for more than 500 cycles at current densities of 1.25 and 10 mA  $\text{cm}^{-2}$ . However, the  $\text{Zn}(\text{CF}_3\text{SO}_3)_2/\text{AN}$  electrolyte showed slightly lower overpotential during the initial cycles and better plating–stripping over long-term cycling. The XPS analysis confirmed that no SEI layer is formed on Zn metal surface after plating–stripping. On the contrary,  $\text{Zn}(\text{TFSI})_2/\text{AN}$

electrolyte displayed better anodic stability on Al current collector where almost no corrosion current was measured up to 2.25 V. The TiN/Ti showed an anodic stability comparable with that of Al current collector. Other investigated current collectors such as C/Al and MWCNT-paper offered an inferior performance compared with Al foil. This work sheds light on the next steps toward the development of full-cell nonaqueous Zn batteries and Zn-ion-based hybrid supercapacitor (Zn-HSC).<sup>[27]</sup>

### Supporting Information

Supporting Information is available from the Wiley Online Library or from the author.

### Acknowledgements

The authors acknowledge the Swedish energy agency, STandUP for Energy, and the Swedish Research Council for Environment, Agricultural Sciences and Spatial Planning (FORMAS) (project number 2016-01257) for financial support. The authors would like to thank Sebastian Grans for technical support.

### Conflict of Interest

The authors declare no conflict of interest.

### Keywords

current collector, nonaqueous electrolytes, plating–stripping, surface analysis, Zn metal

Received: April 18, 2020

Revised: June 16, 2020

Published online: August 5, 2020

- [1] F. Wang, X. Wu, X. Yuan, Z. Liu, Y. Zhang, L. Fu, Y. Zhu, Q. Zhou, Y. Wu, W. Huang, *Chem. Soc. Rev.* **2017**, *46*, 6816.
- [2] M. R. Palacín, *Chem. Soc. Rev.* **2009**, *38*, 2565.
- [3] A. S. Etman, L. Wang, K. Edström, L. Nyholm, J. Sun, *Adv. Funct. Mater.* **2019**, *29*, 1806699.
- [4] A. S. Etman, J. Sun, R. Younesi, *J. Energy Chem.* **2019**, *30*, 145.
- [5] A. S. Etman, H. D. Asfaw, N. Yuan, J. Li, Z. Zhou, F. Peng, I. Persson, X. Zou, T. Gustafsson, K. Edström, J. Sun, *J. Mater. Chem. A* **2016**, *4*, 17988.
- [6] A. S. Etman, Z. Wang, A. El Ghazaly, J. Sun, L. Nyholm, J. Rosen, *ChemSusChem* **2019**, *12*, 5157.
- [7] A. S. Etman, A. K. Inge, X. Jiaru, R. Younesi, K. Edström, J. Sun, *Electrochim. Acta* **2017**, *252*, 254.
- [8] H. Shao, Y. Wu, Z. Lin, P.-L. Taberna, P. Simon, *Chem. Soc. Rev.* **2020**, *49*, 3005.
- [9] N. Nitta, F. Wu, J. T. Lee, G. Yushin, *Mater. Today* **2015**, *18*, 252.
- [10] D. Deng, *Energy Sci. Eng.* **2015**, *3*, 385.
- [11] J. B. Goodenough, K. S. Park, *J. Am. Chem. Soc.* **2013**, *135*, 1167.
- [12] G. E. Blomgren, *J. Electrochem. Soc.* **2017**, *164*, A5019.
- [13] P. Canepa, G. Sai Gautam, D. C. Hannah, R. Malik, M. Liu, K. G. Gallagher, K. A. Persson, G. Ceder, *Chem. Rev.* **2017**, *117*, 4287.
- [14] J. Muldoon, C. B. Bucur, T. Gregory, *Chem. Rev.* **2014**, *114*, 11683.
- [15] W. Kaveevitvachai, A. Manthiram, *J. Mater. Chem. A* **2016**, *4*, 18737.

- [16] J. Zhao, K. K. Sonigara, J. Li, J. Zhang, B. Chen, J. Zhang, S. S. Soni, X. Zhou, G. Cui, L. Chen, *Angew. Chem. Int. Ed.* **2017**, *56*, 7871.
- [17] S.-D. Han, N. N. Rajput, X. Qu, B. Pan, M. He, M. S. Ferrandon, C. Liao, K. A. Persson, A. K. Burrell, *ACS Appl. Mater. Interfaces* **2016**, *8*, 3021.
- [18] J. Ming, J. Guo, C. Xia, W. Wang, H. N. Alshareef, *Mater. Sci. Eng. R: Rep.* **2019**, *135*, 58.
- [19] P. Senguttuvan, S.-D. Han, S. Kim, A. L. Lipson, S. Tepavcevic, T. T. Fister, I. D. Bloom, A. K. Burrell, C. S. Johnson, *Adv. Energy Mater.* **2016**, *6*, 1600826.
- [20] T. J. Simons, M. Salsamendi, P. C. Howlett, M. Forsyth, D. R. Macfarlane, C. Pozo-Gonzalo, *ChemElectroChem* **2015**, *2*, 2071.
- [21] A. Guerfi, J. Trottier, I. Boyano, I. De Meatza, J. A. Blazquez, S. Brewer, K. S. Ryder, A. Vjih, K. Zaghbi, *J. Power Sources* **2014**, *248*, 1099.
- [22] S.-D. Han, S. Kim, D. Li, V. Petkov, H. D. Yoo, P. J. Phillips, H. Wang, J. J. Kim, K. L. More, B. Key, R. F. Klie, J. Cabana, V. R. Stamenkovic, T. T. Fister, N. M. Markovic, A. K. Burrell, S. Tepavcevic, J. T. Vaughey, *Chem. Mater.* **2017**, *29*, 4874.
- [23] M. S. Chae, J. W. Heo, H. H. Kwak, H. Lee, S.-T. Hong, *J. Power Sources* **2017**, *337*, 204.
- [24] C. Pan, R. G. Nuzzo, A. A. Gewirth, *Chem. Mater.* **2017**, *29*, 9351.
- [25] K. Lu, B. Song, Y. Zhang, H. Ma, J. Zhang, *J. Mater. Chem. A* **2017**, *5*, 23628.
- [26] N. Zhang, Y. Dong, Y. Wang, Y. Wang, J. Li, J. Xu, Y. Liu, L. Jiao, F. Cheng, *ACS Appl. Mater. Interfaces* **2019**, *11*, 32978.
- [27] H. Wang, M. Wang, Y. Tang, *Energy Storage Mater.* **2018**, *13*, 1.
- [28] Z. Chen, T. Liu, Z. Zhao, Z. Zhang, X. Han, P. Han, J. Li, J. Wang, J. Li, S. Huang, X. Zhou, J. Zhao, G. Cui, *J. Power Sources* **2020**, *457*, 227994.
- [29] H. S. Kim, T. S. Arthur, G. D. Allred, J. Zajicek, J. G. Newman, A. E. Rodnyansky, A. G. Oliver, W. C. Boggess, J. Muldoon, *Nat. Commun.* **2011**, *2*, 426.
- [30] A. Ponrouch, C. Frontera, F. Bardé, M. R. Palacín, *Nat. Mater.* **2016**, *15*, 169.
- [31] K. Ta, K. A. See, A. A. Gewirth, *J. Phys. Chem. C* **2018**, *122*, 13790.
- [32] D. Enslin, M. Stjern Dahl, A. Nyttén, T. Gustafsson, J. O. Thomas, *J. Mater. Chem.* **2009**, *19*, 82.
- [33] A. Heckmann, J. Thienenkamp, K. Beltrop, M. Winter, G. Brunklaus, T. Placke, *Electrochim. Acta* **2018**, *260*, 514.